PERGAMON

International Journal of Heat and Mass Transfer 45 (2002) 1321–1332

International Journal of HEAT and MASS TRANSFER

www.elsevier.com/locate/ijhmt

Stability of natural convective motion in pure water near 4°C contained in a slot with a moving sidewall

S. Saravanan, P. Kandaswamy *

Department of Mathematics, Bharathiar University, Coimbatore 641 046, Tamil Nadu, India

Received 26 February 2001

Abstract

The stability of plane parallel convective motion in pure water close to its temperature of maximum density is studied. A layer of ice at its melting temperature is assumed to be contained in an inclined slot with a movable sidewall. The convective motion is induced by uniformly distributed heat sources in the layer. The stability boundary depends on the angle of inclination and velocity of the sidewall. In general lower and moderate positive values of *Re* and moderate and higher negative values of *Re* stabilize convection. The competition between the thermal-buoyant, interactive and shear modes of instability is prominent when $-7 \leqslant Re \leqslant 10$.

1. Introduction

An important type of natural convection arises in the presence of heat sources. This type of natural convection in a vertical slot has even velocity and temperature distribution and so differs considerably from that induced by differential heating. The instability in this case develops in the form of a system of eddies at the boundaries between convective counterflows. For low Prandtl numbers, the hydrodynamical nature of opposing convective flows is the cause for instability of basic state in a vertical slot. As the Prandtl number increases, the situation becomes dangerous because of the amplification of disturbances into thermal running waves [1]. This situation depends much on the Prandtl number. On the other hand thermal factors are the most dangerous when the slot is in the horizontal position. Both the above mechanisms are present when the slot is neither aligned nor normal to the gravity.

Stability of a flow driven by combined shear and buoyancy forces is relevant to many industrial and manufacturing processes such as reactor core, extrusion, drawing, etc. Many geophysical phenomena like motion in between earth's tectonic plates are maintained by buoyancy forces, strongly modified by the coexisting shear. If the Reynolds number is large enough and the shear flow is of Poiseuille or mixed Couette–Poiseuille type, a hydrodynamic instability of the shear flow itself can interact with the thermal instability [2]. In this case the marginal curve may have a double minima, one corresponding to each mode of instability. Chen and Hsieh [3] considered the stability of natural convection in a differentially heated vertical slot with a moving sidewall. Their results showed the critical Prandtl number which marks the transition between shear and buoyant modes is strongly dependent on the direction and speed of the sidewall movement. Chen and Chung [4] have given a detailed review on the mixed convection instability in a vertical channel. Chen and Chung [5] concluded that the existence of multiple local minimum wavenumbers are responsible for the sudden jumps of the critical wavenumber and shift of instability type for high Prandtl number fluids. The growth of a double minimum neutral curve because of the magnetic field was also reported by Kolyshkin [6]. Rogers and Yao [7] studied the different types of instability mechanisms that occur during mixed convection, with special reference to the effect of Prandtl number.

The aim of this study is to understand the process of ice melting. Unlike most of the fluids that possess

* Corresponding author. Tel.: +91-422-422222; fax: +91-422-422387.

E-mail addresses: sshravan@lycos.com (S. Saravanan), pgk0@lycos.com (P. Kandaswamy).

0017-9310/02/$ - see front matter
PII: S0017-9310(01)00148-X

Nomenclature

c_p	specific heat capacity
g	acceleration due to gravity
Gr	Grashof number
h	half slot width
j	$= 1$ for water $= 0$ for fluids with linear density variation
k	wavenumber
$\mathbf{k}$	unit vector in the z direction
n	number of collocation points
$\mathbf{n}$	vertical unit vector pointing upwards
p	pressure
Pr	Prandtl number
q	$=Q/(\rho c_p \kappa)$
Q	volume density of internal heat sources
Re	Reynolds number
t	non-dimensional time
T	non-dimensional temperature
u_0	dimensional velocity of the moving side wall
$\mathbf{v}$	non-dimensional velocity vector
x	coordinate axis normal to the slot
z	coordinate axis parallel to the slot

Greek symbols

α	angle of inclination of the slot
β	coefficient of thermal expansion
η_i	$=\beta_{i+1}q^i h^{2i}/(\beta_1 2^i),\ i=1,2,3$
κ	thermal diffusivity
λ	complex eigenvalue
v	kinematic viscosity
ρ	density
Ψ	non-dimensional stream function
∇	Laplacian operator

Superscripts

*	dimensional quantity
(i)	ith derivative

Subscripts

c	critical state
0	basic state

monotonic linearly decreasing density–temperature relationships, water exhibits a non-linear density variation with a maximum at 4°C (more exactly 3.98°C) at atmospheric pressure. This anomalous behaviour of density behaviour greatly affects the freezing of the upper surface of water bodies supporting marine ecology. El-Henaway [8] made a stability analysis in water near its density maximum in the region of buoyancy force reversal. Convective stability of water lying between two vertical plates of different temperatures near its maximum density was first studied by Hassab and Sorour [9]. Farhadieh and Tankin [10] studied the effect of convective current on the ice–water interface, with different salinity concentrations. Other works in fluids with non-linear density include those of Gebhart and Mollendorf [11], Spatz et al. [12], Blake et al. [13] and Merker et al. [14]. Motivated by the above factors, this study considers the linear stability of natural convection generated by internal heat sources in water in the neighbourhood of its density maximum.

2. The equations

Let us consider a slot containing two infinitely long, parallel sidewalls of distance $2h$ (Fig. 1(a)) enclosing ice at its melting temperature 273.15 K ($=0$°C). The temperature of both walls are always kept at 273.15 K. The density–temperature relationship for water is assumed to be (see [15] and Fig. 1(b))

$$\rho = \rho_0(1 + \beta_1 T^* + \beta_2 T^{*2} + \beta_3 T^{*3} + \beta_4 T^{*4}), \tag{1}$$

where $\rho_0 = 999.8396$ is the density of water that occurs at the reference temperature 273.15 K, $\beta_1 = 0.6814493\times 10^{-4}$, $\beta_2 = -0.9160979 \times 10^{-5}$, $\beta_3 = 0.1109033 \times 10^{-6}$ and $\beta_4 = 0.1864194 \times 10^{-8}$. The heating is initiated by internal heat sources of uniform volume density Q distributed uniformly through the volume. It is assumed that the temperature produced by Q is at most 277.15 K ($=4$°C). As a result the solid ice is transformed into water. For small thickness of h, a laminar parallel flow is developed as a result of density difference in the fluid. The slot is inclined to the vertical at an angle α which is positive in the clockwise sense. The left sidewall is moving up at a constant velocity u_0. We choose a Cartesian coordinate system, where the x- and z-axes are normal and parallel to the plates. The origin of the coordinate system is located in the midplane of the slot. The equations governing the motion of a viscous incompressible fluid in the above configuration with the Boussinesq approximation are

$$\begin{aligned}(\partial/\partial t^*)\mathbf{v}^* + (\mathbf{v}^*\cdot\nabla^*)\mathbf{v}^* &= -(1/\rho)\nabla^* p^* + v(\nabla^*)^2\mathbf{v}^* + [(-1)^j\beta_1 T^* - j\beta_2 T^{*2} \\ &\quad - j\beta_3 T^{*3} - j\beta_4 T^{*4}]g\mathbf{n},\end{aligned} \tag{2}$$

$$(\partial/\partial t^*)T^* + (\mathbf{v}^*\cdot\nabla^*)T^* = \kappa(\nabla^*)^2 T^* + (Q/\rho c_p), \tag{3}$$

$$\operatorname{div}\mathbf{v}^* = 0, \tag{4}$$

where $j = 1$ for water and 0 for fluids with linear density variation.

We introduce the non-dimensional variables $x = x^*/h$, $z = z^*/h$, $t = t^*/(h^2/v)$, $\mathbf{v} = \mathbf{v}^*/(g\beta_1 q h^4/2v)$, $p =$

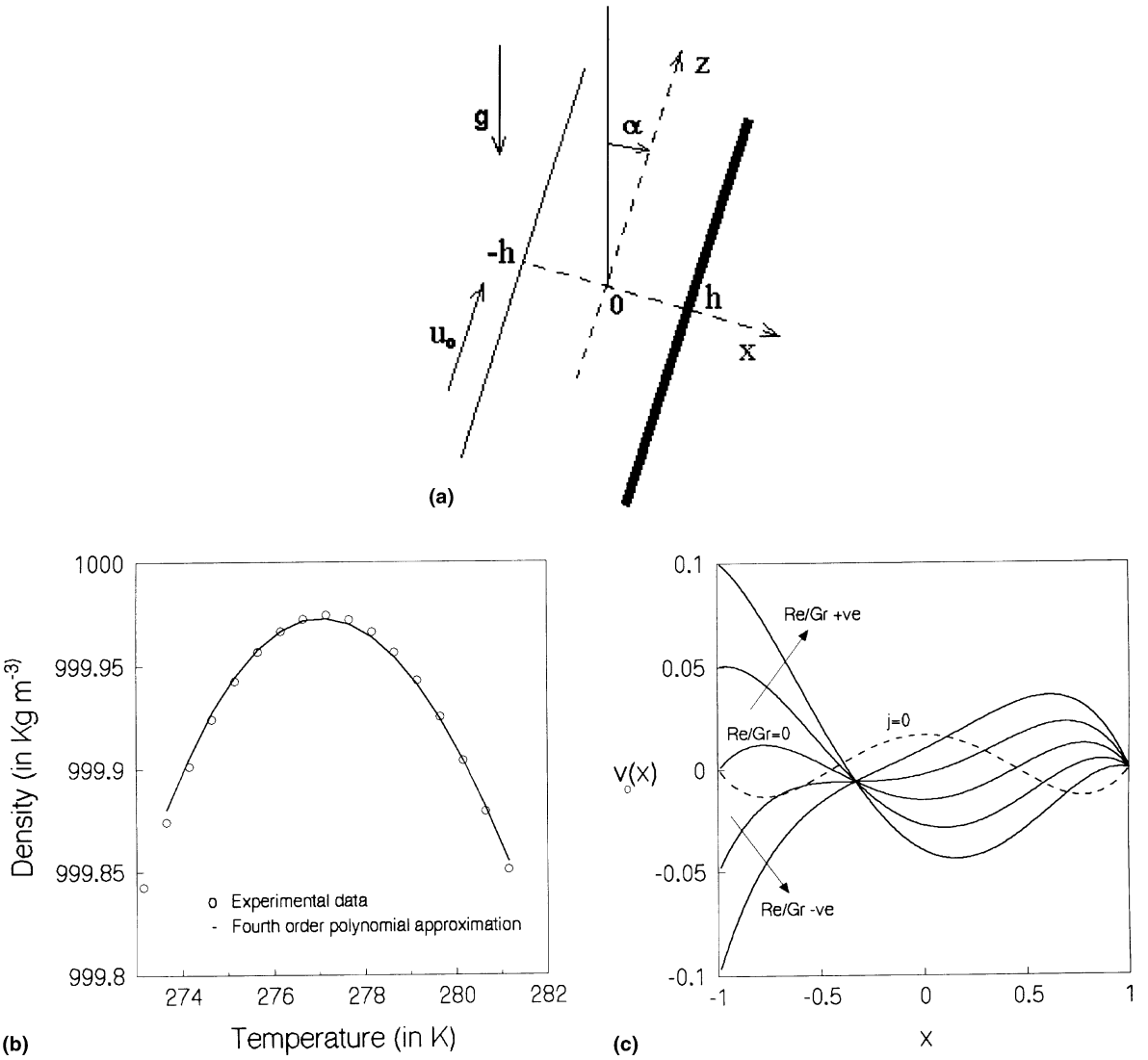

Fig. 1. (a) Physical schematic. (b) Non-linear density behaviour of water. (c) Basic velocity profiles for $j = 1$ and $\alpha = 0°$.

$p^*/(\rho g\beta_1 h^3/2)$, $T = T^*/(qh^2/2)$. Let $Gr = g\beta_1 qh^5/2\nu^2$ be the Grashof number, $Re = u_0 h/\nu$ the Reynolds number, $Pr = \nu/\kappa$ the Prandtl number and $q = Q/(\rho c_p \kappa)$. In dimensionless variables, Eqs. (2)–(4) become

$$(\partial/\partial t)\mathbf{v} + Gr(\mathbf{v}\cdot\nabla)\mathbf{v} = -\nabla p + \nabla^2\mathbf{v} + [(-1)^j T - j\eta_1 T^2 - j\eta_2 T^3 - j\eta_3 T^4]\mathbf{n}, \tag{5}$$

$$(\partial/\partial t)T + Gr(\mathbf{v}\cdot\nabla)T = (1/Pr)\nabla^2 T + q, \tag{6}$$

$$\text{div } \mathbf{v} = 0, \tag{7}$$

where

$$\eta_i = \frac{\beta_{i+1} q^i h^{2i}}{\beta_1 2^i} \quad (i = 1, 2, 3),$$

$\mathbf{v}$, T, p and $\mathbf{n}$ are, respectively, the velocity of the fluid, temperature, pressure and vertical unit vector. We seek a steady plane parallel solution for Eqs. (5)–(7) of the following type:

$$\mathbf{v} = [0, 0, v_0(x)], \quad T = T_0(x), \quad p = p_0(z). \tag{8}$$

The flow (8), may be realized in the middle portion of a sufficiently long vertical layer of fluid where the end effects are negligible. Substituting (8) into (5)–(7) leads to the system

$$d^2 v_0/dx^2 = C + \left[(-1)^{j+1} T_0 + j\eta_1 T_0^2 + j\eta_2 T_0^3 + j\eta_3 T_0^4\right]\cos\alpha, \tag{9}$$

$$d^2T_0/dx^2 = -2 \tag{10}$$

subjected to the boundary conditions

$$v_0(+1) = 0, \quad v_0(-1) = Re/Gr, \quad T_0(\pm 1) = 0. \tag{11}$$

The solution at the basic state is given by

$$v_0(x) = C(x^2-1)/2 + Re/(2Gr) + C_1 - Rex/(2Gr) + C_2x^2 + C_3x^4 + C_4x^6 + C_5x^8 + C_6x^{10}, \tag{12}$$

$$T_0(x) = 1 - x^2, \tag{13}$$

where

$$\begin{aligned}
C_1 &= (-(1+\eta_1+\eta_2+\eta_3)/2 + (1+2\eta_1+3\eta_2+4\eta_3)/12 \\
&\quad - (\eta_1+3\eta_2+6\eta_3)/30 + (\eta_2+4\eta_3)/56 - \eta_3/90)\cos\alpha, \\
C_2 &= ((1+\eta_1+\eta_2+\eta_3)/2)\cos\alpha, \\
C_3 &= (-(1+2\eta_1+3\eta_2+4\eta_3)/12)\cos\alpha, \\
C_4 &= ((\eta_1+3\eta_2+6\eta_3)/30)\cos\alpha, \\
C_5 &= (-(\eta_2+4\eta_3)/56)\cos\alpha, \\
C_6 &= (\eta_3/90)\cos\alpha.
\end{aligned}$$

We consider the case of a closed channel. This warrants the fluid through the cross-section of the channel to be zero and hence

$$\int_{-1}^{1} v_0(x)\,dx = 0. \tag{14}$$

The symmetric basic flow for $\alpha = 0°$ and $Re/Gr = 0$ consists of three streams: two upstreams at the boundaries and a central downstream (Fig. 1(c)). When α is non-zero, we observe a reduction in the basic velocity from (12). When Re/Gr is non-zero the velocity profiles are no longer symmetric. The downward movement of the wall ($Re/Gr < 0$) is associated with the formation of a boundary layer near the moving wall.

We consider the stability of the above basic state by the method of small perturbations. Let us consider the perturbed motion $\mathbf{v}_0 + \mathbf{v}$, $T_0 + T$, and $p_0 + p$, where $\mathbf{v}$, T and p are small unsteady perturbations, $\mathbf{v}_0 = v_0\mathbf{k}$. The perturbation in the velocity component v_y is equal to zero and the other components v_x, v_z, and perturbations of T and p do not depend on y (so called plane perturbations). Then Eqs. (5)–(7) for the above perturbed state after linearization take the form:

$$\begin{aligned}
&(\partial/\partial t)\mathbf{v} + Gr[(\mathbf{v}_0\cdot\nabla)\mathbf{v} + (\mathbf{v}\cdot\nabla)\mathbf{v}_0] \\
&\quad = -\nabla p + \nabla^2\mathbf{v} + \left[(-1)^j T - 2j\eta_1 T_0 T \right. \\
&\qquad \left. - 3j\eta_2 T_0^2 T - 4j\eta_3 T_0^3 T\right]\mathbf{n},
\end{aligned} \tag{15}$$

$$(\partial/\partial t)T + Gr(\mathbf{v}_0\cdot\nabla)T + (\mathbf{v}\cdot\nabla)T_0 = (1/Pr)\nabla^2 T, \tag{16}$$

$$\operatorname{div}\mathbf{v} = 0. \tag{17}$$

It is convenient to introduce the stream function $\Psi(x,z)$ as

$$v_x = -\partial\Psi/\partial z, \quad v_z = \partial\Psi/\partial x. \tag{18}$$

We set

$$\begin{aligned}
\Psi(x,z,t) &= \phi(x)\exp(-\lambda t + \mathrm{i}kz), \\
T(x,z,t) &= \theta(x)\exp(-\lambda t + \mathrm{i}kz),
\end{aligned} \tag{19}$$

where ϕ and θ are the amplitudes of the normal perturbations, k is the wavenumber and λ is a complex eigenvalue. Substituting (19) in (15)–(17), we obtain the amplitude equations

$$\begin{aligned}
&\phi^{(4)} - 2k^2\phi^{(2)} + k^4\phi + \mathrm{i}kGr\left[v_0^{(2)}\phi - v_0(\phi^{(2)} - k^2\phi)\right] \\
&\quad - \left[-(-1)^j\theta^{(1)} + 2j\eta_1 T_0\theta^{(1)} + 2j\eta_1 T_0^{(1)}\theta \right. \\
&\quad + 3j\eta_2 T_0^2\theta^{(1)} + 6j\eta_2 T_0 T_0^{(1)}\theta + 4j\eta_3 T_0^3\theta^{(1)} + 12j\eta_3 T_0^2 T_0^{(1)}\theta\Big] \\
&\quad \times\cos\alpha - \left[-(-1)^j\mathrm{i}k\theta + 2\mathrm{i}kj\eta_1 T_0\theta + 3\mathrm{i}kj\eta_2 T_0^2\theta \right. \\
&\quad \left. + 4\mathrm{i}kj\eta_3 T_0^3\theta\right]\sin\alpha \\
&\quad = \lambda\left(k^2\phi - \phi^{(2)}\right),
\end{aligned} \tag{20}$$

$$(1/Pr)\left(\theta^{(2)} - k^2\theta\right) + \mathrm{i}kGr\left(T_0^{(1)}\phi - v_0\theta\right) = -\lambda\theta. \tag{21}$$

The velocity and temperature perturbations vanish at the sidewalls and hence the boundary conditions are

$$\phi(\pm 1) = 0, \quad \phi^{(1)}(\pm 1) = 0, \quad \theta(\pm 1) = 0. \tag{22}$$

3. Method of solution

We solve the boundary value problem by the spectral collocation method of Kolyshkin and Vaillancourt [16] for the solution of Orr–Sommerfeld problem. We introduce the fundamental interpolation polynomials

$$\begin{aligned}
P_n(x,\Phi) &= \sum_{j=1}^{n} p_{nj}(x)\phi_j, \\
Q_n(x,\Phi) &= \sum_{j=1}^{n} q_{nj}(x)\phi_j, \\
S_n(x,\Phi) &= \sum_{j=1}^{n} s_{nj}(x)\phi_j, \\
U_n(x,\Theta) &= \sum_{j=1}^{n} p_{nj}(x)\theta_j, \\
V_n(x,\Theta) &= \sum_{j=1}^{n} q_{nj}(x)\theta_j,
\end{aligned} \tag{23}$$

where $\Phi = (\phi_1,\ldots,\phi_n)^{\mathrm{T}} \in R^n$, $\Theta = (\theta_1,\ldots,\theta_n)^{\mathrm{T}} \in R^n$, $\phi(j) = \phi(x_j)$ and $\theta_j = \theta(x_j)$ and

$$p_{nj}(x) = T_n(x)/((x-x_j)T_n^{(1)}(x_j)),$$
$$q_{nj}(x) = p_{nj}(x)(1-x^2)/(1-x_j^2), \quad (24)$$
$$s_{nj}(x) = q_{nj}(x)(1-x^2)/(1-x_j^2).$$

Here $T_n(x)$ denotes the Chebyshev polynomial of the first kind of degree n whose zeroes are $x_j = \cos((2j-1)\pi/2n)$, $j = 1, \ldots, n$. One can easily verify that $S_n(x, \Phi)$ and $V_n(x, \Theta)$ satisfy the boundary conditions (22) for ϕ and θ, respectively.

Substitution of (23) in (20) and (21) leads to the system of equations

$$\sum_{j=1}^{n} \phi_j \left[s_{nj}^{(4)}(x) + a_1(x) q_{nj}^{(2)}(x) + a_2(x) p_{nj}(x) \right] + \sum_{j=1}^{n} \theta_j \left[\left(a_3(x) p_{nj}^{(1)}(x) + a_4(x) p_{nj}(x) \right) \cos\alpha + a_5(x) p_{nj}(x) \sin\alpha \right] = 0, \quad (25)$$

$$\sum_{j=1}^{n} \phi_j b_1(x) p_{nj}(x) + \sum_{j=1}^{n} \theta_j \left[q_{nj}^{(2)}(x) + b_2(x) p_{nj}(x) \right] = 0, \quad (26)$$

where

$$a_1(x) = -2k^2 - \mathrm{i}kGrv_0(x) + \lambda,$$
$$a_2(x) = \mathrm{i}kGrv_0^{(2)}(x) + \mathrm{i}k^3 Grv_0(x) + k^4 - k^2\lambda,$$
$$a_3(x) = (-1)^j - 2j\eta_1 T_0 - 3j\eta_2 T_0^2 - 4j\eta_3 T_0^3,$$
$$a_4(x) = -2j\eta_1 T_0^{(1)} - 6j\eta_2 T_0 T_0^{(1)} - 12j\eta_3 T_0^2 T_0^{(1)},$$
$$a_5(x) = (-1)^j \mathrm{i}k - 2j\mathrm{i}k\eta_1 T_0 - 3j\mathrm{i}k\eta_2 T_0^2 - 4j\mathrm{i}k\eta_3 T_0^3,$$
$$b_1(x) = \mathrm{i}kGrPrT_0^{(1)}$$
$$b_2(x) = -k^2 - \mathrm{i}kGrPrv_0 + \lambda Pr$$

Thus, we obtain a finite dimensional eigenvalue problem $(\mathbf{A} - \lambda\mathbf{B})\mathbf{u} = \mathbf{0}$, where $\mathbf{u} = (\phi_1, \ldots, \phi_n, \theta_1, \ldots, \theta_n)'$.

The eigenvalues of the matrix produced by the spectral method are determined by a complex QZ method [17]. A computer code was written to implement this using the algorithm of Golub and Van Loan [18]. The method is very stable and required computer time is moderate. The advantages of the method are the numerical results provide a global instability and no initial guesses are required. The real parts of the eigenvalues $R\lambda_i$, determine the stability of the flow. If $R\lambda_i > 0$ for all i, the flow is stable. If $R\lambda_i < 0$ for at least one value of i, the flow is unstable. The marginal stability curve corresponds to the case when one of the eigenvalues satisfies $R\lambda = 0$. The system depends on many parameters, namely Gr, Re, α, Pr, η_i $(i = 1, 2, 3)$, k, and n. As the interest is on the sidewall movement in an inclined configuration, both q and h in η_i are fixed as unity. To locate an extremal point we proceed as follows. For fixed values of the other parameters, we determine the Grashof number $Gr(k)$ as a function of the wavenumber k corresponding to the case $R\lambda = 0$. Then the critical Grashof number is found by setting $Gr_c = \min_k Gr(k)$.

The convergence of the numerical solution has been checked by varying the number of collocation points n. Table 1 shows the critical states for different combinations. We noticed that at $n = 11$ the 0.5% convergence criterion is met. Further increase in n considerably increases the cost. So we fixed n as 11 in our calculations. Table 2 compares the critical states based on our code for different values of Pr and $j = 0$ with those of Gershuni et al. [1]. They used approximating polynomials of different lengths in their Galerkin's method and so their results differ slightly. Still we observe a good agreement between the results at the same conditions which provide a further check on the numerical accuracy.

4. Results and discussion

First of all let us deal with fluids having linear density variation ($j = 0$). The effect of Pr on the marginal stability curve is shown in Fig. 2(a). For a low Pr approximation (i.e., at $Pr = 0.01$), the neutral curve A has a single minimum. Since the low Pr fluids are good conductors of heat, they immediately dissipate the temperature disturbances before the disruption of buoyancy force to cause instability. Hence the instability causing the single minimum by the unstable velocity distribution is referred to as shear (S) mode. On the other hand as Pr increases, the penetration depth of temperature disturbances decreases, and hence the

Table 1
Critical Grashof number for different n ($j = 1$ and $Pr = 12.97$)

n	$\alpha = 0°$, $Re = 0$	$\alpha = 30°$, $Re = -25$	$\alpha = -60°$, $Re = -10$	$\alpha = 5°$, $Re = 5$
6	121.68	161.29	139.33	292.14
7	197.50	404.00	163.70	321.75
8	164.27	270.97	157.76	275.95
9	157.92	316.72	159.36	268.96
10	154.12	351.40	159.23	262.05
11	153.73	350.43	159.25	261.35

Table 2
Comparison of the present results ($j = 0,\ \alpha = 0°,\ Re = 0$) with those of Gershuni et al. [1] (within parentheses)

Pr	Gr_c	k_c
0.01	1690.75	2.06
(0)	(1720)	(2.05)
0.4	1213.53	1.65
	(1219)	(1.65)
1	730.32	1.37
	(744)	(1.38)
2	457.77	1.35
	(470)	(1.35)
3	348.59	1.34
	(359)	(1.35)
5	250.86	1.36
	(259)	(1.35)
10	165.26	1.36
	(171)	(1.38)
20	111.77	1.39
	(115)	(1.40)

buoyant force becomes more concentrated resulting in an instability. In Fig. 2(a) we see that the critical Grashof number Gr_c is considerably lowered with a corresponding shift towards the lower wavenumber region even for $Pr = 1$. Further increase in Pr results in the development of a nose shaped piece, labelled as B, in the curve in the lower wavenumber region. This converts the neutral curve into two branches, having a local minimum in each branch separated by a local maximum. Hence the nose shaped part of neutral curve represents the difference between full stability problem and the Orr–Sommerfeld problem for the same velocity profiles. Accordingly the marginal wavespeed becomes bimodal as shown in Fig. 2(b). The wavespeed is measured in the same units as the velocity of the base flow and is normalized by the modulus of maximum velocity of base flow: $c = \mathrm{Im}(\lambda)/kGrv_{0\max}$, where λ is a purely imaginary eigenvalue and $v_{0\max}$ is the absolute value of the maximum non-dimensional velocity. Perturbations in the form of thermal running waves with comparatively high phase velocity correspond to the nose shaped lower part, and hence this branch is associated with thermal-buoyant (TB) mode of instability [19]. So depending on Pr, two modes of instability can occur: S-mode and TB-mode.

We shall now investigate the effect of sidewall movement of a vertical slot containing water ($j = 1$, $Pr = 12.97$). The considerable distortion of the marginal stability curve appearing with increasing Re is noticeable in Fig. 3(a). The marginal curve has two branches marked A and B corresponding to S- and TB-modes, as discussed above. When Re becomes 5, another branch develops in the marginal curve marked by C and blends together smoothly with the other two branches. The instability giving birth to this branch receiving energy partly from the buoyant force and partly from the mainstream velocity by the Reynolds stress is referred to as interactive (I) mode. Then the absolute minimum of these three branches decides the stability behaviour. The corresponding marginal phase velocity is considerably lowered with three distinct branches as shown in Fig. 3(c). When Re is increased further to 10, the disturbances receive more energy by the action of Reynolds stress between the up and downstream convective flows. Hence the branch C elongates in the downward direc-

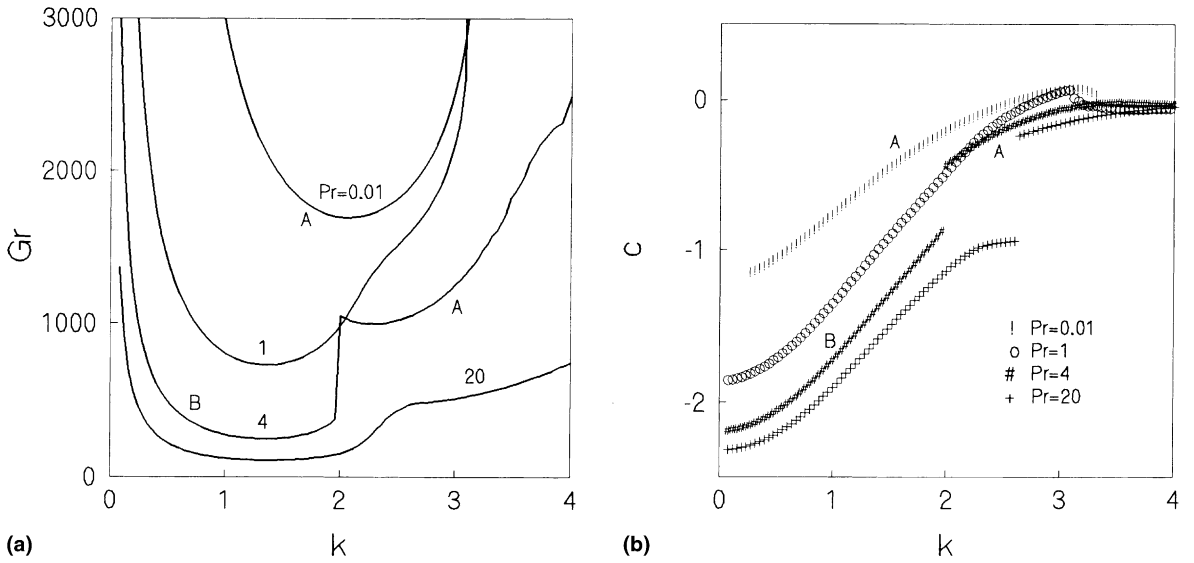

Fig. 2. (a) Marginal stability curves for $j = 0$, $\alpha = 0°$, $Re = 0$ varying Pr. (b) Marginal wavespeeds for $j = 0$, $\alpha = 0°$, $Re = 0$ varying Pr.

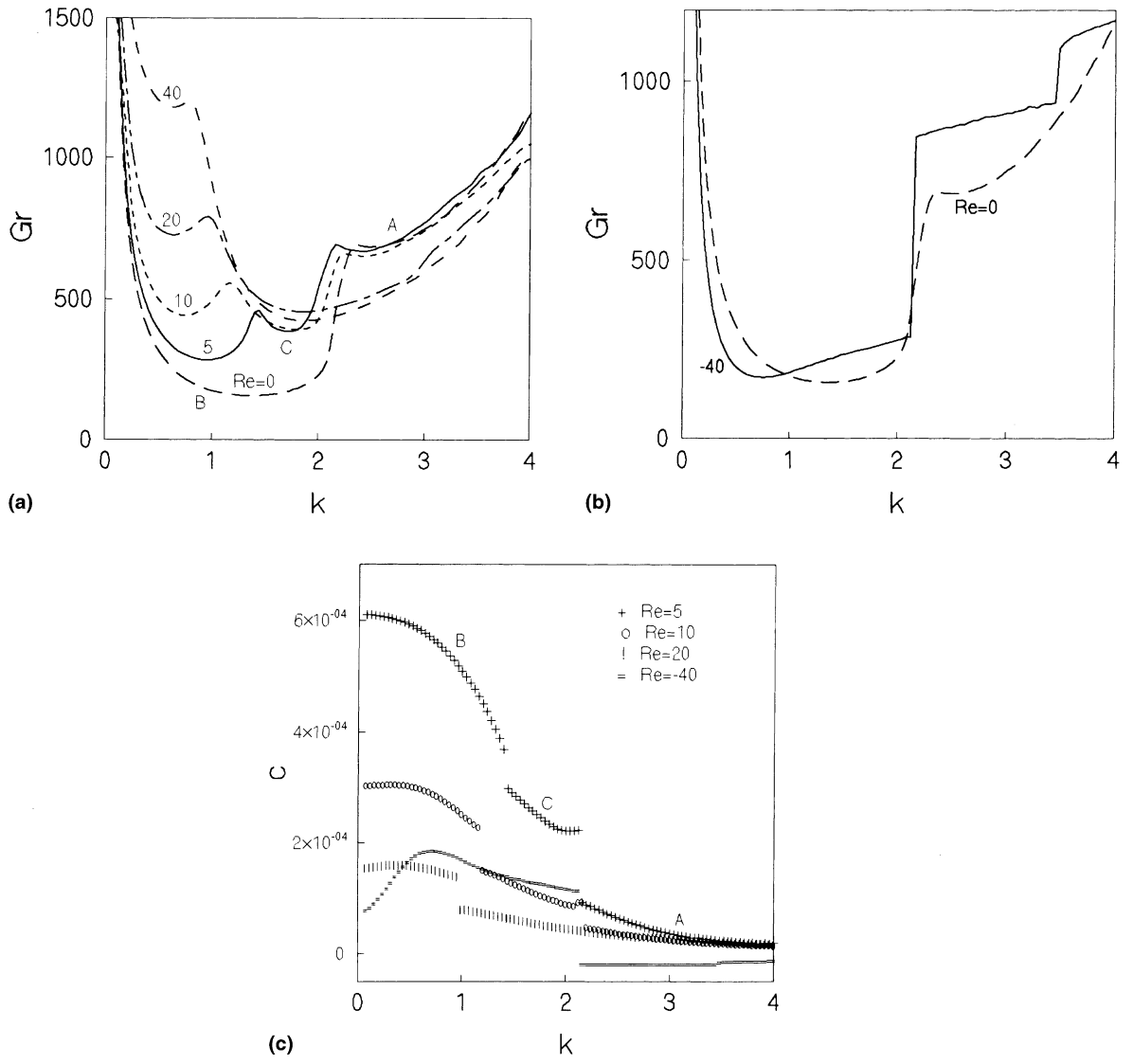

Fig. 3. (a) Marginal stability curves for $j = 1$, $Pr = 12.97$, $\alpha = 0°$ varying Re ($Re \geqslant 0$). (b) Marginal stability curves for $j = 1$, $Pr = 12.97$, $\alpha = 0°$ varying Re ($Re \leqslant 0$). (c) Marginal wavespeeds for $j = 1$, $Pr = 12.97$, $\alpha = 0°$ varying Re.

tion dominating branch B and hence decides the stability behaviour. For further increase in Re, branch C disappears and branch A begins to dominate (see Fig. 3(c)). Ultimately the effect of upward movement of the sidewall is to stabilize the basic flow up to $Re = 24$ beyond which the flow gets destabilized. But when the wall starts moving in the downward direction, the situation is completely different. Formation of a boundary layer on the moving sidewall becomes prominent for higher negative values of Re. This inhibits the development of Reynolds stress and hence the source of energy to disturbances is buoyant in nature. Thus decrease in the value of Re is associated with TB-mode as shown in Fig. 3(b).

The stability boundary of convective motion in water contained in a vertical slot is shown in (Re, Gr_c) plane (Fig. 4(a)). The dashed line represents that of a fluid with linear density variation. We observe that convection is stabilized for $0 < Re < 24$, with a sharp increase in Gr_c up to $Re = 8.4$. This sharp increase in Gr_c occurs while TB-mode remaining critical after competing with I- or S-mode. For higher Re ($Re > 24$), the convective motion is destabilized. Negative values of Re do not have comparatively much influence on the stability of the basic flow. However, lower negative values of Re ($-20 > Re > 0$) slightly destabilize the flow whereas higher negative values start stabilizing. The critical wavenumber k_c corresponding to the secondary flow at

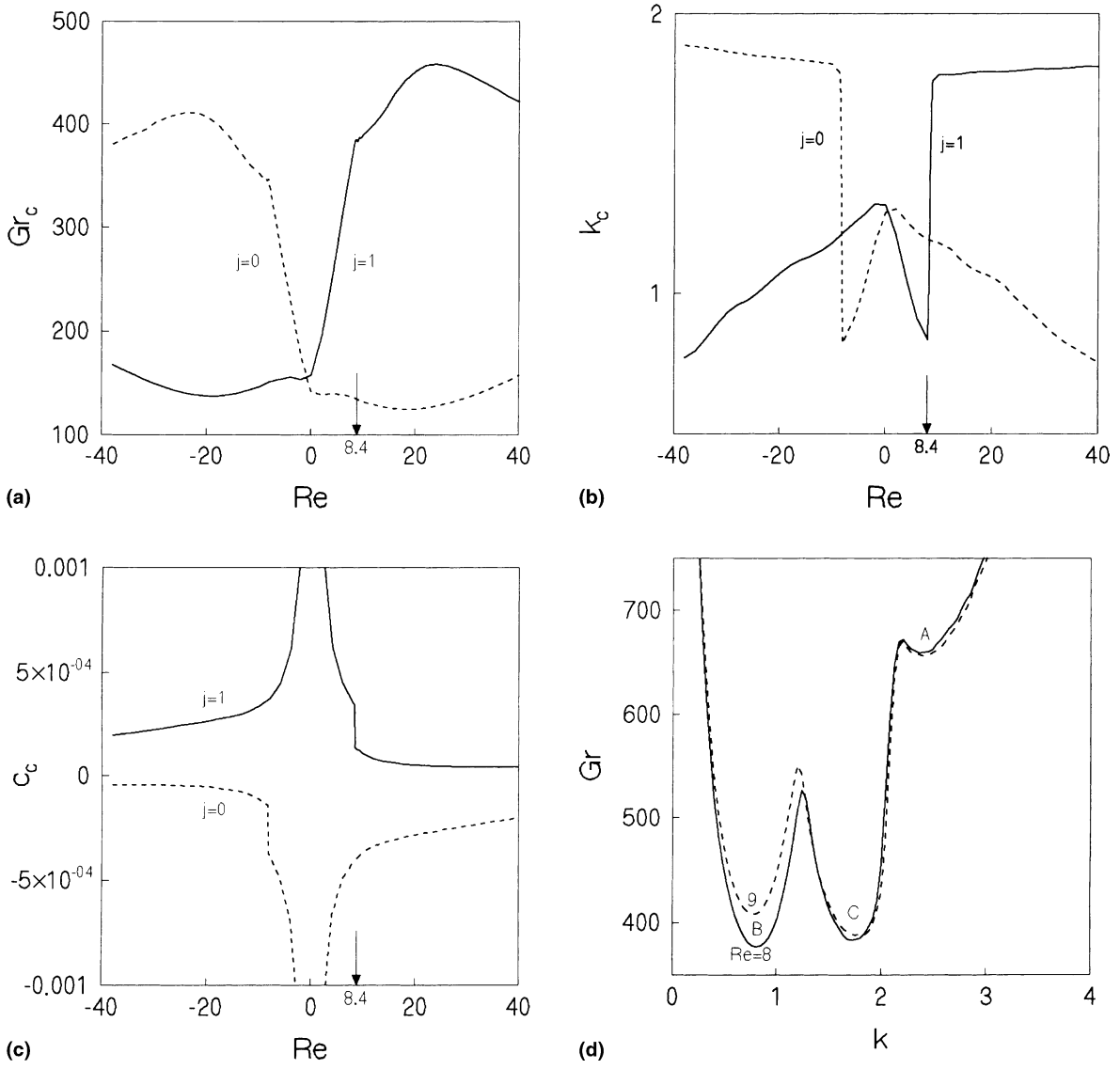

Fig. 4. Effect of sidewall movement in a vertical slot ($j = 1$): (a) Gr_c against Re. (b) k_c against Re. (c) c_c against Re. (d) Marginal curves exhibiting change in the critical mode.

the neutral state is displayed in Fig. 4(b). The wavenumber decreases sharply for $0 < Re < 8.4$ corresponding to the sharp increase in Gr_c and then a jump occurs at $Re = 8.4$ shifting the wavenumber to some higher value. This jump corresponds to the transition of absolute minimum from TB- to I-mode as shown in Fig. 4(d). Physically this means a sudden change in the vertical cell size. This is analogous to those arising in our previous result [20]. Thus in general a jump in the wavenumber corresponds to an abrupt transition of global minimum from one branch of the neutral curve to the neighboring one. And a sharp decrease in wavenumber before the jump indicates the emergence and growth of a new branch in the neutral curve to which the absolute minimum gets transferred immediately after the jump. A more or less opposite behaviour is observed for fluids with $j = 0$. The dependence of the critical wavespeed c_c of the perturbation upon Re is shown in Fig. 4(c). As $|Re|$ increases from 0, the velocity of upward moving perturbations decreases with a jump discontinuity at $Re = 8.4$. We observe that perturbations travel downward for $j = 0$.

Let us now concentrate on non-vertical slots. We allowed α to vary as 15°, 30°, 45° and 60° in both directions for investigating the effect of sidewall movement. The critical Grashof number, wavenumber and

wavespeed against *Re* for positive angles of tilt are shown in Fig. 5(a)–(c), respectively. In all cases, the effect of *Re* is to stabilize convection for $Re < -20$ and $0 \leqslant Re \leqslant 20$. In general for positive values of *Re*, the flow stabilizes up to $\alpha = 30°$ and then starts destabilizing for higher α. This shows somewhat a non-linear dependence of the stability behaviour for positive values of *Re*. On the other hand for negative values of *Re*, the basic state is destabilized when α increases. When α becomes 15°, the jump in k_c is advanced to $Re = 6.8$ which shows that the Reynolds stress due to oppositely moving convective patterns is increasing. When α is increased to 30°, jumps in k_c corresponding to the two sudden changes in the directions of Gr_c at $Re = 3.8$ and 16.6 are introduced. These two jumps result because of the shifting of the global minimum from the first branch (corresponding to TB-mode) to the third (corresponding to S-mode) via the second one (corresponding to I-mode) as shown in Figs. 7(a) and (b). But only one jump is seen in k_c for higher values of α because of the disappearance of I-mode branch as shown in Fig. 5(b). The corresponding wavespeeds show an interesting result. When *Re* remains positive and α becomes 30° or more, the travelling perturbations suddenly change their direction and move with gravity. Reduction in wavespeed is clear for increasing $|Re|$. But no such direction-change is observed in the case when $Re < 0$. Fig. 5 (d) shows a closer look at the jumps occurring in wavespeed.

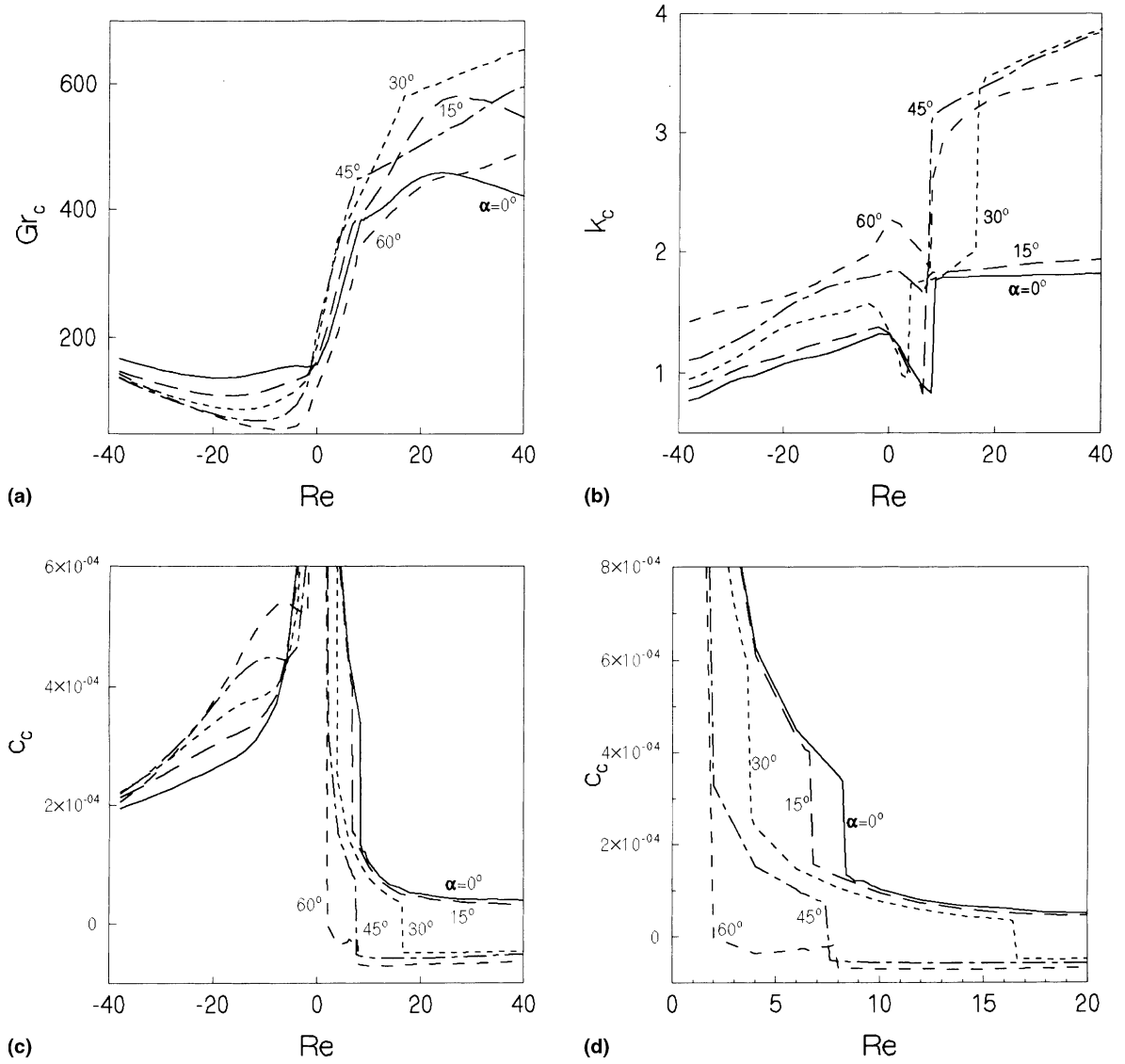

Fig. 5. Effect of sidewall movement in a positively inclined slot ($j = 1$): (a) Gr_c against *Re*. (b) k_c against *Re*. (c) and (d) c_c against *Re*.

Somewhat complicated behaviour occurs in (Gr_c, Re) plane (Fig. 6(a)) for smaller values of $|Re|$ in the case of negative tilt angles. Although we observe a complicated feature in Gr_c, the gross effect shows the destabilizing and stabilizing phenomena for positive and negative values of Re, respectively, as α is increased. When the sidewall is moving up, negative inclination produces a non-linear effect on the mode-changing phenomenon, i.e., the jump from TB- to I- or S-mode gets delayed as α decreases up to $-30°$ and then starts advancing. When the sidewall is moving down, the critical S-mode is completely replaced by I-mode. A competition occurs between TB- and I-modes for negative values of Re when α reaches $-15°$. Here we observe a sharp increase in k_c and then an immediate fall at $Re = -6.4$. This develops into a peak at $Re = -4$ for $\alpha = -30°$. For further decrease in α, the peak at a negative Re and the jump at a positive Re become closer showing more competition between TB, I and S modes. The marginal curves for selected values of Re at $\alpha = -45°$ display this behaviour (see Fig. 7(c)). This shows a close interlocking of the two different instability mechanisms namely sidewall movement and tilt. The wavespeeds in Fig. 6(c) and (d) show some jumps corresponding to those occurring in k_c. Here also the perturbation speed decreases as the speed of sidewall starts increasing. Negative wavespeeds are seen for larger tilt angles and $Re < 0$. The effect of tilting the slot when the sidewall is moving

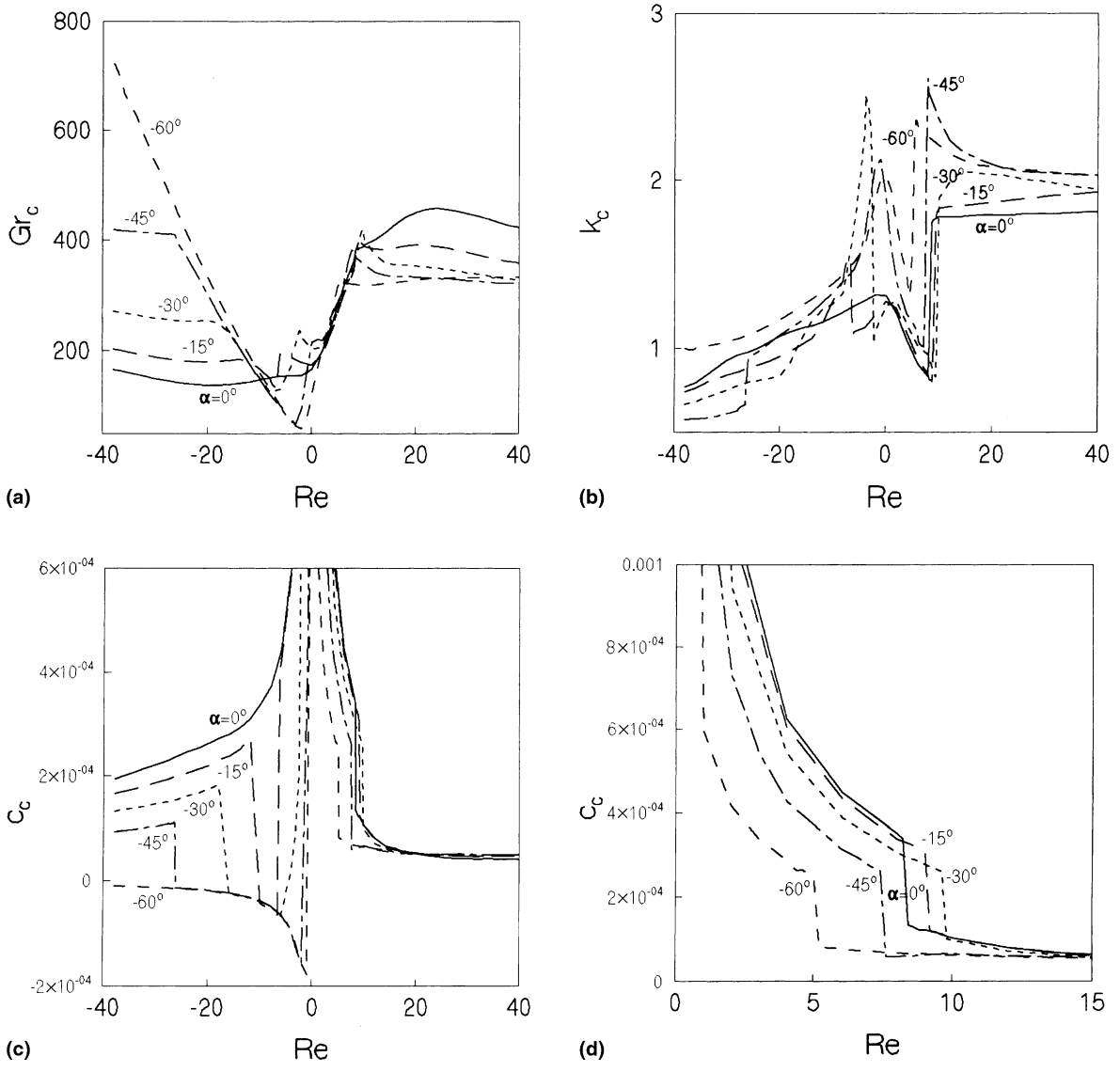

Fig. 6. Effect of sidewall movement in a negatively inclined slot ($j = 1$): (a) Gr_c against Re. (b) k_c against Re. (c) and (d) c_c against Re.

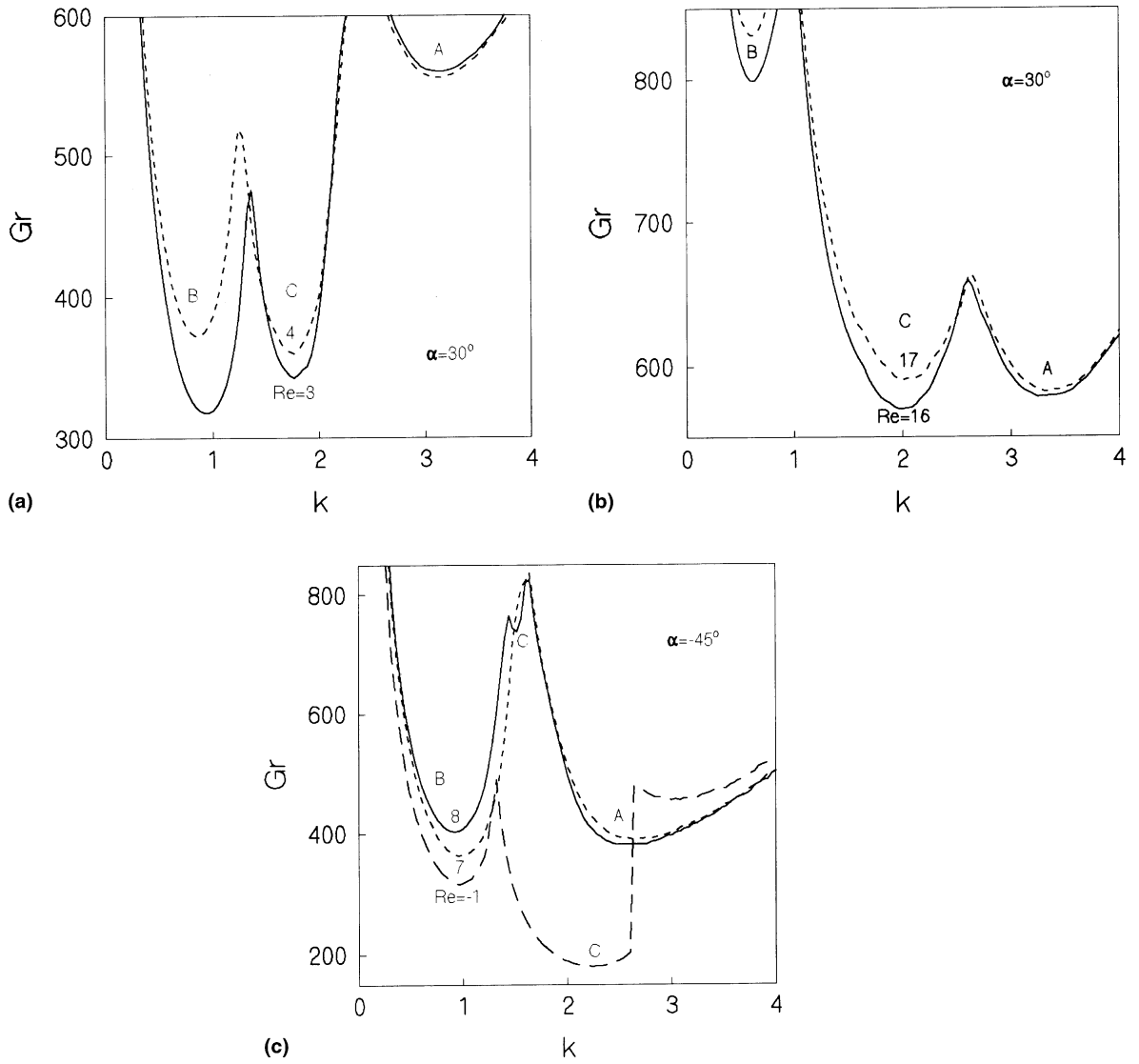

Fig. 7. Marginal curves for inclined slots ($j = 1$): (a) $\alpha = 30°$ and $Re = 3, 4$. (b) $\alpha = 30°$ and $Re = 16, 17$. (c) $\alpha = -45°$ and $Re = -1, 7, 8$.

at a constant velocity is exhibited in Fig. 8. The positive values of Re stabilizes the convective flow, whereas higher negative values of Re stabilizes for $\alpha < 0$ and destabilizes for $\alpha > 0$. The sharp increase in Gr_c for $Re = -5$ near $\alpha = -30°$ is because of the emergence of I-mode in the critical phenomenon, as seen in Fig. 6(b).

5. Conclusion

The onset of instability of the combined natural forced convective flow in water contained in a slot is greatly dependent on α and Re. The critical boundary for water is more or less opposite in nature compared to that of fluids with linear density variation. Upward movement of the sidewall stabilizes convection until $Re = 24$ in the case of a vertical slot. On the other hand, the birth of S-mode gets inhibited for higher negative values of Re. The stability of the basic flow is found to be a non-linear function of α reaching a maximum at $\alpha = 30°$ for $Re > 0$. In general destabilization is found for increasing values of α and $Re < 0$. When α takes negative values, somewhat complicated behaviour occurs in Gr_c. In this case, we observe more competition among the different modes causing instability for $-7 \leqslant Re \leqslant 10$, accompanied by jumps in k_c.

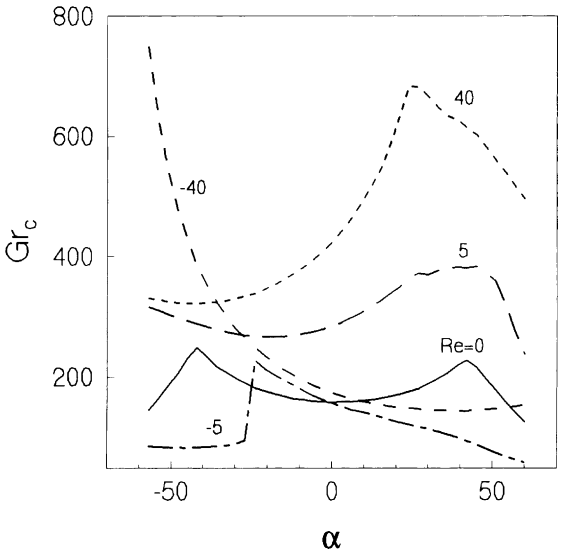

Fig. 8. Effect of tilting the slot ($j = 1$).

Acknowledgements

One of the authors (S.S.) thanks CSIR, India for its financial support through Senior Research Fellowship (NET).

References

[1] G.Z. Gershuni, E.M. Zhukhovitskii, A.A. Iakimov, Two kinds of instability of stationary convective motion induced by internal heat sources, Sov. J. Appl. Math. Mech. 37 (1973) 544–548.

[2] A.A. Mohammad, R. Viskanta, Stability of lid driven shallow cavity heated from below, Int. J. Heat Mass Transfer 32 (1989) 2155–2166.

[3] J.C. Chen, C.K. Hsieh, Linear stability of natural convection in a tall vertical slot with a moving sidewall, Int. J. Heat Mass Transfer 36 (1993) 1471–1476.

[4] Y.C. Chen, J.N. Chung, The linear stability of mixed convection in a vertical channel flow, J. Fluid Mech. 325 (1996) 29–51.

[5] Y.C. Chen, J.N. Chung, Stability of mixed convection in a differentially heated vertical channel, ASME – J. Heat Transfer 120 (1998) 127–132.

[6] A.A. Kolyshkin, On the stability of steady convective motion generated by heat sources in a magnetic field, Can. J. Phys. 66 (1988) 990–993.

[7] B.B. Rogers, L.S. Yao, The importance of Prandtl number in mixed convection instability, ASME – J. Heat Transfer 115 (1993) 482–486.

[8] I.M. El-Henaway, A stability analysis of non-time-periodic perturbations of buoyancy induced flows in pure water near 4°C, J. Fluid Mech. 163 (1985) 1–20.

[9] M.A. Hassab, M.M. Sorour, Onset of convection in a melted ice layer between vertical plates, Int. J. Heat Mass Transfer 25 (1982) 909–916.

[10] R. Farhadieh, R.S. Tankin, A study of freezing of sea water, J. Fluid Mech. 71 (1975) 293–304.

[11] G. Gebhart, J.C. Mollendorf, Buoyancy induced flows in a liquid under conditions in which density extrema may arise, J. Fluid Mech. 9 (1978) 673–707.

[12] T.L. Spatz, D. Poulikakos, M.J. Kazmierczak, High Reynolds number experiments in a horizontal layer of water around its density maximum, ASME – J. Heat Transfer 111 (1989) 578–581.

[13] K.R. Blake, D. Poulikakos, A. Bejan, Natural convection near 4°C in a horizontal layer heated from below, Phys. Fluids 27 (1984) 2608–2616.

[14] G.M. Merker, P. Waas, U. Grigull, Onset of convection in a horizontal water layer with maximum density effects, Int. J. Heat Mass Transfer 22 (1979) 505–515.

[15] B. Gebhart, Y. Jaluria, R.L. Mahajan, B. Sammakia, Buoyancy Induced Flows and Transports, reference ed., Hemisphere, Washington, 1988.

[16] A.A. Kolyshkin, R. Vaillancourt, On the stability of nonisothermal circular Couette flow, Phys. Fluids A 5 (1993) 3136–3146.

[17] C.B. Moler, G.W. Stewart, An algorithm for generalized matrix eigenvalue problems, SIAM J. Numer. Anal. 10 (1973) 241–256.

[18] G.H. Golub, C.F. Van Loan, Matrix Computations, II ed., North Oxford Academic Publishing, Oxford, 1986.

[19] J.E. Hart, Stability of the flow in a differentially heated inclined box, J. Fluid Mech. 47 (1971) 547–576.

[20] S. Saravanan, P. Kandaswamy, Stability of natural convective motion induced by internal heat sources in a slot with a moving sidewall, Acta Mechanica (in press).